A Letters Journal Exploring the Frontiers of Physics

October 2010

EPL, **92** (2010) 20007
doi: 10.1209/0295-5075/92/20007

www.epljournal.org

Conditional measurements on multimode pairwise entangled states from spontaneous parametric downconversion

A. Allevi[1], A. Andreoni[1,2], F. A. Beduini[4], M. Bondani[1,3], M. G. Genoni[4,5], S. Olivares[4,5] and M. G. A. Paris[4,5(a)]

[1] *CNISM UdR Como - I-22100 Como, Italia, EU*
[2] *Dipartimento di Fisica e Matematica, Università degli Studi dell'Insubria - I-22100 Como, Italia, EU*
[3] *Istituto di Fotonica e Nanotecnologie - CNR-IFN - I-22100, Como, Italia, EU*
[4] *Dipartimento di Fisica dell'Università degli Studi di Milano - I-20133 Milano, Italia, EU*
[5] *CNISM, UdR Milano Università - I-20133 Milano, Italia, EU*

received 21 June 2010; accepted in final form 8 October 2010
published online 15 November 2010

PACS 03.67.Bg – Entanglement production and manipulation
PACS 42.50.Dv – Quantum state engineering and measurements
PACS 03.65.Wj – State reconstruction, quantum tomography

Abstract – We address the intrinsic multimode nature of the quantum state of light obtained by pulsed spontaneous parametric downconversion and develop a theoretical model based only on experimentally accessible quantities. We exploit the pairwise entanglement as a resource for conditional multimode measurements and derive closed formulas for the detection probability and the density matrix of the conditional states. We present a set of experiments performed to validate our model in different conditions that are in excellent agreement with experimental data. Finally, we evaluate the non-Gaussianity of the conditional states obtained from our source with the aim of discussing the effects of the different experimental parameters on the effectiveness of this type of conditional state preparation.

Nonclassical states of the radiation field are a crucial ingredient for fundamental tests of quantum mechanics and represent a resource for quantum communication and high-precision measurements. In fact, much attention has been devoted to their generation schemes. Besides squeezing, nonclassical effects are generally observed in connection with non-Gaussian states of light, and this usually implies the presence of fluctuating parameters [1,2] or the use of nonlinearities higher than second order, *e.g.* the Kerr effect [3–5]. On the other hand, the reduction postulate provides an alternative mechanism to achieve effective nonlinear dynamics. In fact, if a measurement is performed on a portion of a composite entangled system, the other component is conditionally reduced according to the outcome of the measurement. The resulting dynamics may be highly nonlinear, and may produce quantum states that cannot be generated by currently achievable nonlinear processes [6]. The efficiency of the process, *i.e.* the rate of success in getting a certain state, is equal to the probability of obtaining a certain outcome from the measurement and it may be higher than nonlinear efficiency, thus making conditional schemes possibly convenient even when a corresponding Hamiltonian process exists.

The nonlinear dynamics induced by conditional measurements has been analyzed for a large variety of schemes [6–27], including photon addition and subtraction schemes [8–10,12,13], optical state truncation of coherent states [14], generation of cat-like states [15–17], state filtering by active cavities [18,19], synthesis of arbitrary unitary operators [20] and generation of optical qubit by conditional interferometry [21]. More recently, nonGaussian states and operations have been studied in connection with entanglement distillation [28–31], teleportation [8–10], cloning [32] and quantum storage [33]. Conditional state generation has been achieved in the low energy regime [34–39] by using single-photon detectors and time-multiplexed photon resolving ones [36], and a question arises on whether photon counting may be exploited on multimode correlated states in the mescoscopic regime.

In this paper we address multimode conditional measurements and demonstrate a novel bright source of

(a) E-mail: matteo.paris@fisica.unimi.it

conditional states [40] based on i) pulsed multimode spontaneous parametric downconversion (PDC) [41–48], which produces entangled states with a mesoscopic number of photons and ii) a conditional intensity measurement performed by photoemissive detectors, called hybrid photodetectors, that are able to partially resolve the number of detected photons [49]. We develop a theoretical model based only on experimentally accessible quantities and derive closed formulas for both the detection probabilities and the conditional states. We find an excellent agreement with the experimental data and succeed in evaluating the amount of non-Gaussianity of the conditional states despite the multimode character of the entangled state.

The pair of intense correlated beams obtained by pulsed PDC represents a convenient system for state preparation by conditional measurements. In this case, the state outgoing the crystal is intrinsically multimode because of the pulsed nature of the pump and the properties of the nonlinear interaction [43,50], whereas correlations are provided by the pairwise entanglement induced by spontaneous PDC. If we assume that the output energy is equally distributed among the μ modes of each beam, then the overall multimode state produced by pulsed PDC can be written as a tensor product of μ identical twin-beam states, *i.e.*,

$$\boldsymbol{R} = \bigotimes_{k=1}^{\mu} |\lambda\rangle\!\rangle_{kk}\langle\!\langle\lambda|,$$
$$|\lambda\rangle\!\rangle = \sqrt{1-\lambda^2}\sum_n \lambda^n |n\rangle\otimes|n\rangle$$

with $\lambda^2 = N/(\mu+N)$, N being the mean total number of photons in either of the two beams. In our scheme, which is sketched in fig. 1, conditional preparation is obtained when one of the two beams undergoes a photon counting process. If we assume that the detector efficiency η is the same for each of the μ modes, the probability operator-valued measure (POVM) $\{\boldsymbol{\Pi}_m\}$ describing the detection of m photoelectrons may be written as

$$\boldsymbol{\Pi}_m = \sum_{\boldsymbol{q}} \delta_{m\gamma} \bigotimes_{j=1}^{\mu} \Pi_{q_j},$$

where $\mathbf{q} = \{q_1, \ldots, q_\mu\}$, $\gamma = \sum_{k=1}^{\mu} q_k$, δ_{hk} is the Kronecker delta, and

$$\Pi_q = \eta^q \sum_{k=q}^{\infty} (1-\eta)^{k-q} \binom{k}{q} |k\rangle\langle k|$$

denotes the single-mode photon counting POVM. The joint probability distribution of photoelectrons is given by $p_{12}(s,t) = \mathrm{Tr}_{12}[\boldsymbol{R}\,\boldsymbol{\Pi}_s \otimes \boldsymbol{\Pi}_t]$, that, after some algebra, reads

$$p_{12}(s,t) = \left(\frac{\mu\eta}{M+\mu\eta}\right)^{\mu} \left(\frac{\eta}{1-\eta}\right)^{s+t} \times \sum_{l=\max(s,t)}^{\infty} \left[\frac{M(1-\eta)^2}{M+\mu\eta}\right]^{l} \binom{l+\mu-1}{l} \binom{l}{s} \binom{l}{t}, \quad (1)$$

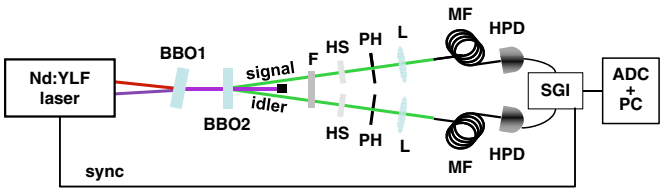

Fig. 1: (Color online) Schematic diagram of the experimental setup. BBO1 and BBO2: nonlinear crystals; F: cut-off filter; HS: harmonic separators; PH: pin-hole apertures; L: lenses; MF: multimode optical fibers; HPD: amplified hybrid photodetectors; SGI: synchronous gated integrator; PC: digitizing PC board.

where $M = \frac{1}{2}\mathrm{Tr}_{12}[\boldsymbol{R}\sum_s s\,\boldsymbol{\Pi}_s \otimes \sum_t t\,\boldsymbol{\Pi}_t] = \eta N$ is the total mean number of photoelectrons measured on each of the two beams. Notice that (1) only contains quantities that can be experimentally accessed by direct detection.

When one beam is detected, say the idler, and t photoelectrons are obtained in the measurement, the corresponding conditional state of the signal is given by $\varrho_t = 1/p_2(t)\mathrm{Tr}_2[\boldsymbol{R}\,\mathbb{I}\otimes\boldsymbol{\Pi}_t]$ where $p_2(t) = \sum_s p_{12}(s,t)$ is the marginal probability of measuring t photoelectrons on the idler beam. After some calculations we arrive at

$$\varrho_t = \sum_{\boldsymbol{q}} w_t(\gamma)\,\theta(\gamma-t) \bigotimes_{k=1}^{\mu} |q_k\rangle\langle q_k|,$$

where $\theta(x)$ is the Heaviside step function,

$$w_t(\gamma) = \binom{\gamma}{t} \frac{\eta^t (M_t - t\eta)^\gamma}{(M_t+\mu\eta)^\gamma [p_2(t)\,(1+M/\eta\mu)^\mu\,(1-\eta)^t]}$$

and

$$M_t = \mathrm{Tr}_1\left[\varrho_t \sum_s s\boldsymbol{\Pi}_s\right] = [t(M+\eta\mu) + \mu M(1-\eta)](M+\mu)^{-1}$$

is the mean number of photoelectrons for the conditional state ϱ_t. Similarly, upon selecting a set of possible results $t \in \mathcal{T}$ according to a given rule $\mathcal{T}$, a suitable engineering of the conditional state $\varrho_{\mathcal{T}}$ may be achieved. As an example, we will consider the states

$$\varrho_*^{(\pm)} = \sum_{t \gtrless t^*} p_2(t)\,\varrho_t$$

obtained by keeping the photoelectrons on the idler that are larger or smaller than a given threshold t^*.

The experimental setup is sketched in fig. 1. The light source was a Nd:YLF ps-pulsed laser (High-Q Laser Production, Austria) with built-in second and third harmonic generation. The output at the fundamental (1047 nm) and that at the third harmonics (349 nm) were used to produce a UV pump field (261.75 nm) via noncollinear sum frequency generation in a BBO crystal (β-BaB_2O_4, Castech, China, cut angle 37°, 8 mm thick). The pump was then sent into another BBO crystal

(Kaston, China, cut angle 48.84°, 4 mm length) to produce pairwise entanglement at 523.5 nm, in order to match the peak quantum efficiency ($\eta \sim 50\%$) of our hybrid photodetectors (HPD, R10467U-40, Hamamatsu, Japan). The UV stray light was cut-off by a filter and by two harmonic separators. Signal and idler were selected by two pinholes (PH of 200 or 300 μm diameter in fig. 1), located at 1 m distance from the nonlinear crystal (BBO2) in order to minimize the number of collected modes. Notice that the number of temporal modes, which is evaluated from the marginal detected-photon number distribution, cannot be reduced at will. The only way to reduce the number of modes is to select a single spatial mode, which involves the challenging matching of the collection areas in signal and idler. The possible mismatch between the collection areas results in an effective detection efficiency, reduced in comparison to the nominal efficiency of the detectors, which can be estimated through the level of noise reduction $R = \sigma^2(s-t)/\langle s+t\rangle = 1-\eta$ [43] exhibited by two beams. For our beams we obtain, without noise subtraction, $\eta \sim 0.06$. The light passing the pin-holes was coupled to two multimode optical fibers and delivered to the detectors, whose outputs were amplified (preamplifier A250 plus amplifier A275, Amptek), synchronously integrated (SGI, SR250, Stanford), digitized (ATMIO-16E-1, National Instruments) and, finally, processed off-line. Each experimental run was performed on 50 000 subsequent laser shots at fixed values of the pump intensity.

HPD detectors, which play a crucial role in our conditional scheme, are endowed with a partial photon number resolving power, that allows the recognition of a few number of detected-photon peaks in their output. HPD detectors proved to be useful in reconstructing the detected-photon number distributions of a number of optical states without any *a priori* knowledge of it [49,51] and the shot-by-shot detected-photon number correlations [52]. To achieve these results, a novel method to analyze the output signal of linear detectors with high gain has been developed [53]. The primary photon-detection process (*e.g.* photoelectron emission) is described by a Bernoullian convolution, whereas the overall amplification and conversion process is assumed to correspond to a convolution with the amplification lineshape of the detection [53]. Actually, the amplification process may be described by a single multiplicative factor, γ, if the single-photoelectron response of the detector is well separated from the zero-peak, which is the case of our HPD detectors [53]. With these assumptions, the statistics of the output of the detection apparatus (voltages, v, in the present case) can be linked to that of the detected photons. In particular, we can write the mean value as $\overline{v} = \gamma\overline{m} = \eta\gamma\overline{n}$, η being the overall detection efficiency, and the variance as $\sigma^2(v) = \gamma^2\sigma^2(m) = \gamma^2(\eta^2\sigma^2(n) + \eta(1-\eta)\overline{n})$. By writing the Fano factor of the output voltages as $F_v = \sigma^2(v)/\overline{v} = (Q/\overline{n})\overline{v} + \gamma$, we find a linear dependence on $\overline{v}$ and observe that the dependence on the field under investigation is only in the angular coefficient, $Q/\overline{n}$, where Q is the Mandel parameter. Thus, by measuring the F_v at different values of $\overline{v}$, we can obtain γ from a fit of the experimental data. Once γ is evaluated, it is possible to find the detected-photon distribution by dividing the v output values by the experimental value of γ and re-binning the data in unitary bins [49,51]. Moreover, we demonstrated that by directly assigning the value of the bin, that is the specific number of detected photons, to the shot-by-shot value of the output v, we actually could correctly evaluate photon number correlations [52]. Here, we exploit HPD detectors to perform both conclusive and inconclusive conditional measurements of the photon number statistics [13].

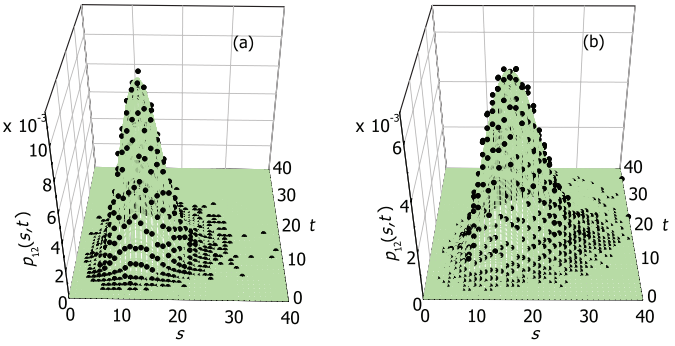

Fig. 2: (Color online) Joint probability distribution of photoelectrons $p_{12}(s,t)$ compared to the experimental points. (a) $\mu = 197$, $\eta = 0.06$ and $M = 13.4$; (b) $\mu = 25$, $\eta = 0.056$ and $M = 17.1$.

As a first test of the correctness of our multimode description we checked the expression of $p_{12}(s,t)$ against data: in fig. 2 we report the experimental joint probability distribution superimposed to the theoretical one, evaluated for the experimental values of the parameters (panel (a): PH = 200 μm, $\mu = 197$, $\eta = 0.06$ and $M = 13.4$; panel (b): PH 300 μm, $\mu = 25$, $\eta = 0.056$ and $M = 17.1$). The experimental results fit the theory very well and the fidelity $\sum_{st}\sqrt{p_{12}^{th}(s,t)p_{12}^{exp}(s,t)}$ exceeds 0.99 for the whole range of parameters. We also notice that the marginal probability distributions $p_1(s)$ and $p_2(s)$ are multithermal distributions as it has been already observed in experiments performed at different intensity regimes [43,49,50].

In fig. 3 we report the photon distributions $p_{1|2}(s|\mathcal{T}) = \mathrm{Tr}_1[\varrho_{\mathcal{T}}\,\mathbf{\Pi}_s]$ of conditional states as obtained from the state in fig. 2(a) by choosing the values of the measured photons on the idler beam according to a given rule and selecting the corresponding ensemble on the signal beam. Panel (a) of fig. 3 displays the distributions for the detected photons state ϱ_t obtained by choosing a definite number of detected photons ($t = 10$ and $t = 15$); panel (b) those for $\varrho_*^{(+)}$, obtained by keeping the values of detected photons larger than a threshold t^* ($t^* = 11$ and $t^* = 17$); finally, panel (c) those for $\varrho_*^{(-)}$ ($t^* = 8$ and $t^* = 15$). We notice that i) the results are in excellent agreement with

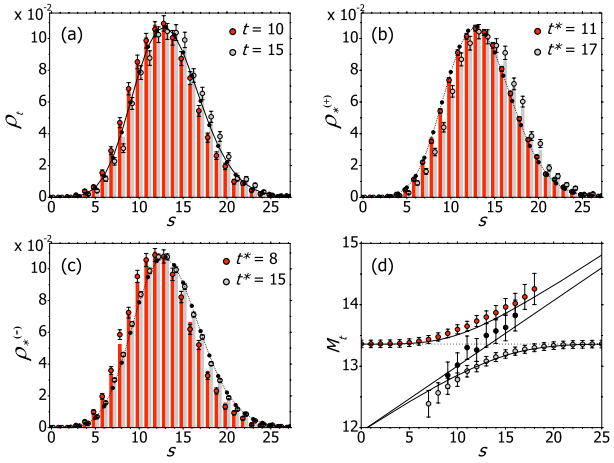

Fig. 3: (Color online) Photon distribution for conditional states. (a) Experimental results (points) and theoretical distribution (histograms) for the photoelectrons in the conditional signal state ϱ_t for $t=10$ (red histogram) and $t=15$ (gray histogram). The black line and the full circles represent, respectively, the theoretical and experimental distribution for the unconditional state. (b) As in panel (a) for $\varrho_*^{(+)}$, $t^*=11$ (red) and $t^*=17$ (gray). (c) As in panel (a) for $\varrho_*^{(-)}$, $t^*=8$ (red) and $t^*=15$ (gray). (d) Experimental mean value of the distributions as a function of the conditioning value (or threshold). Black circles refer to ϱ_t, red circles to $\varrho_*^{(+)}$ and gray circles to $\varrho_*^{(-)}$. Solid lines are the theoretical predictions obtained for M_t. The dashed line corresponds to the mean value of the unconditioned state. The other involved parameters are: $\mu=197$, $\eta=0.06$ and $M=13.4$.

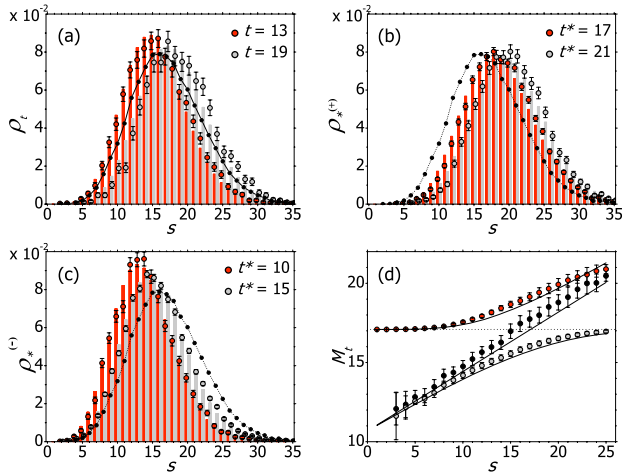

Fig. 4: (Color online) Photon distribution for conditional states. (a) Experimental results (points) and theoretical distribution (histograms) for the photoelectrons in the conditional signal state ϱ_t for $t=13$ (red histogram) and $t=19$ (gray histogram). The black line and the full circles represent, respectively, the theoretical and experimental distribution for the unconditional state. (b) As in panel (a) for $\varrho_*^{(+)}$, $t^*=17$ (red) and $t^*=21$ (gray). (c) As in panel (a) for $\varrho_*^{(-)}$, $t^*=10$ (red) and $t^*=15$ (gray). (d) Experimental mean value of the distributions as a function of the conditioning value (or threshold). Black circles refer to ϱ_t, red circles to $\varrho_*^{(+)}$ and gray circles to $\varrho_*^{(-)}$. Solid lines are the theoretical predictions obtained for M_t. The dashed line corresponds to the mean value of the unconditioned state. The other involved parameters are: $\mu=25$, $\eta=0.056$ and $M=17.1$.

theory and ii) despite the small value of effective quantum efficiency the "conditioning power" of the measurement (*i.e.* the differences between the conditional states and the corresponding original ones) is appreciable. This is clearly illustrated by the behavior of the mean values of the distributions, which are reported in panel (d) of fig. 3 as a function of either the conditioning value or the threshold: the experimental data are in excellent agreement with the predictions for M_t.

In fig. 4 we show the results for a different dataset having similar mean value and a considerably lower number of modes. We note that the results are again in excellent agreement with theory and that we have a greater "conditioning power" compared to the dataset with a larger number of modes.

As an application of our model, we have evaluated the amount of non-Gaussianity of the conditional states. Indeed, the non-Gaussian character of the conditional states may be foreseen from the deviation of the detected-photon statistics from that of the original state. However, the shape of the distributions (not too different from the unconditioned ones) and the low value of the quantum efficiency anticipate that the amount of non-Gaussianity will be unavoidably small. In order to assess the performances of our scheme we focus on the conditional state ϱ_t and use the non-Gaussianity measure $\delta[\varrho]=S[\tau]-S[\varrho]$, where $S[\varrho]$ is the Von Neumann entropy of the state ϱ and τ is the Gaussian reference state of ϱ, *i.e.*, a Gaussian state with the same mean value and covariance matrix as ϱ. δ has been proved to be a proper measure of non-Gaussianity [54], as well as a critical parameter to asses non-Gaussianity as a resource [55]. In our case τ is a factorized thermal state with $M_t/\eta\mu$ mean photons per mode [54] and the Von Neumann entropy of the conditional state is given by $S[\varrho_t]=-\sum_{\gamma=0}^{\infty}\binom{\gamma+\mu-1}{\gamma}w_t(\gamma)\log w_t(\gamma)$. By using the above expression and the Von Neumann entropy of a factorized thermal state, we evaluate the non-Gaussianity and normalize its value to that of a maximally non-Gaussian state for the same mean number of photons and modes, *i.e.*, a factorized Fock state [54]. The renormalized non-Gaussianity $\delta_R[\varrho_t]$ is reported in fig. 5 for different values of the experimental parameters.

As is apparent from the plots the renormalized non-Gaussianity δ_R is a decreasing function of the energy of the conditional state and of the number of modes. The effect of the quantum efficiency is more relevant for large number of modes and large energy. As it concerns the conditioning value t of detected photons, we see that δ_R monotonically increases with t, again with the quantum efficiency playing a major role for large number of modes. Overall, the goal of achieving high non-Gaussianity requires a small number

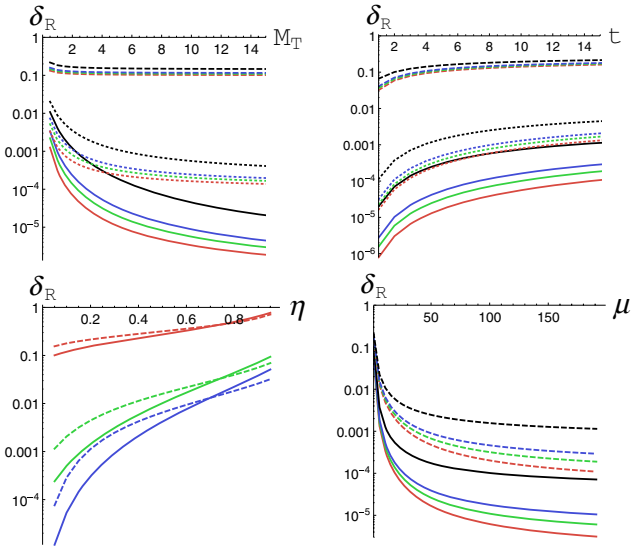

Fig. 5: (Color online) Renormalized non-Gaussianity δ_R of the conditional state ϱ_t for different values of the experimental parameters. Top left panel: δ_R as a function of the total number of measured photoelectrons M_t for $t=5$ and for different values of the quantum efficiency η and of the number of modes μ. Solid lines are for $\mu=197$, dotted lines for $\mu=25$ and dashed lines for $\mu=1$. For each group of lines we have, from bottom to top, $\eta=6\%$ (red), $\eta=8\%$ (green), $\eta=10\%$ (blue) and $\eta=20\%$ (black). Top right panel: δ_R as a function of the conditioning number t of detected photoelectrons on the idler beam for $M_t=4$ and for different values of the quantum efficiency η and of the number of modes μ. Solid lines are for $\mu=197$, dotted lines for $\mu=25$ and dashed lines for $\mu=1$. For each group of lines we have, from bottom to top, $\eta=6\%$ (red), $\eta=8\%$ (green), $\eta=10\%$ (blue) and $\eta=20\%$ (black). Bottom left panel: δ_R as a function of the quantum efficiency η for $M_t=4$ and for different values of the conditioning number t of detected photoelectrons and of the number of modes μ. Solid lines are for $t=5$ and dashed ones for $t=15$. From bottom to top we can see lines for $\mu=197$ (blue), $\mu=25$ (green), and $\mu=1$ (red). Bottom right panel: δ_R as a function of the number of modes μ for $M_t=4$ and for different values of conditioning number t of detected photoelectrons and for the quantum efficiency η. Solid lines are for $t=2$ and dashed lines for $t=15$. For each group of lines we have, from bottom to top, $\eta=6\%$ (red), $\eta=8\%$ (green), $\eta=10\%$ (blue) and $\eta=20\%$ (black).

of modes or, at fixed number of modes, a high value of the quantum efficiency. Since the pulsed nature of the PDC pump unavoidably leads to a multimode output, the performances of the present source in the generation of non-Gaussian states may be improved either by increasing the overall quantum efficiency, *i.e.*, the matching of the collection areas in signal and idler beams or by a suitable source engineering of PDC output [56].

In conclusion, we have suggested and demonstrated a novel bright source of conditional states based on multimode spontaneous PDC and intensity measurements. We have developed a theoretical model based only on experimentally accessible quantities and derived closed formulas for the detection probability, the conditional states and the corresponding non-Gaussianity. We have compared our predictions with experimental data and found an excellent agreement in the whole range of accessible experimental parameters. Our results clearly indicate the possibility of quantum state engineering with multiphoton/multimode conditional states using mesoscopic photon counting and multimode pairwise correlated states.

* * *

This work has been partially supported by the CNR-CNISM agreement. MGAP thanks S. Cialdi, D. Brivio (UniMI), M. Genovese, I. Degiovanni (INRIM - Torino), P. Giorda and M. Allegra (ISI - Torino) for useful discussions.

REFERENCES

[1] D'Auria V., de Lisio C., Porzio A., Solimeno S., Anwar J. and Paris M. G. A., *Phys. Rev. A*, **81** (2010) 033846.
[2] Chiummo A., De Laurentis M., Porzio A., Solimeno S. and Paris M. G. A., *Opt. Express*, **13** (2005) 948.
[3] Silberhorn C., Lam P. K., Weiß O., König F., Korolkova N. and Leuchs G., *Phys. Rev. Lett.*, **86** (2001) 4267.
[4] Glöckl O., Andersen U. L. and Leuchs G., *Phys. Rev. A*, **73** (2006) 012306.
[5] Tyc T. and Korolkova N., *New J. Phys.*, **10** (2008) 023041.
[6] Paris M. G. A., Cola M. and Bonifacio R., *Phys. Rev. A*, **67** (2003) 042104.
[7] D'Ariano G. M., Kumar P., Macchiavello C., Maccone L. and Sterpi N., *Phys. Rev. Lett.*, **83** (1999) 2490.
[8] Opatrný T., Kurizki G. and Welsch D.-G., *Phys. Rev. A*, **61** (2000) 032302; Dakna M., Knöll L. and Welsch D.-G., *Opt. Commun.*, **145** (1998) 309.
[9] Cochrane P. T., Ralph T. C. and Milburn G. J., *Phys. Rev. A*, **65** (2002) 062306.
[10] Olivares S., Paris M. G. A. and Bonifacio R., *Phys. Rev. A*, **67** (2003) 032314; Olivares S. and Paris M. G. A., *J. Opt. B*, **7** (2005) S392.
[11] Olivares S. and Paris M. G. A., *J. Opt. B*, **7** (2005) 616; Invernizzi C., Olivares S., Paris M. G. A. and Banaszek K., *Phys. Rev. A*, **72** (2005) 042105.
[12] Marek P. and Filip R., *Phys. Rev. A*, **81** (2010) 022302.
[13] Allevi A., Andreoni A., Bondani M., Genoni M. G. and Olivares S., *Phys. Rev. A*, **82** (2010) 013816.
[14] Pegg D. T., Philips L. S. and Barnett S. M., *Phys. Rev. Lett.*, **81** (1998) 1604.
[15] Dakna M., Anhut T., Opatrny T., Knöll L. and Welsch D. G., *Phys. Rev. A*, **55** (1997) 3184.
[16] Dakna M., Clausen J., Knöll L. and Welsch D.-G., *Acta Phys. Slovaca*, **48** (1998) 207.
[17] Zheng S. B., *Phys. Lett. A*, **245** (1998) 11.
[18] D'Ariano G. M., Maccone L., Paris M. G. A. and Sacchi M. F., *Phys. Rev. A*, **61** (2000) 053817; *Fortschr. Phys.*, **48** (2000) 511.
[19] Duan Lu-Ming, Giedke G., Cirac J. I. and Zoller P., *Phys. Rev. Lett.*, **84** (2000) 4002.

[20] Hladky B., Drobny G. and Buzek V., *Phys. Rev. A*, **61** (2000) 022102.
[21] Paris M. G. A., *Phys. Rev. A*, **62** (2000) 033813.
[22] Clausen J., Dakna M., Knöll L. and Welsch D.-G., *J. Opt. B*, **1** (1999) 332; Paris M. G. A., *Phys. Lett. A*, **217** (1996) 78.
[23] Napoli A., Messina A. and Maniscalco S., *Acta Phys. Slovaca*, **50** (2000) 519.
[24] Plastina F. and Piperno F., *Eur. Phys. J. D*, **5** (1999) 411.
[25] Ban M., *Opt. Commun.*, **143** (1997) 225.
[26] Kozhekin A., Kurizky G. and Sherman B., *Phys. Rev. A*, **54** (1996) 3535.
[27] Kim M. S., *J. Phys. B*, **41** (2008) 133001.
[28] Eisert J., Scheel S. and Plenio M. B., *Phys. Rev. Lett.*, **89** (2002) 137903.
[29] Fiurášfiek J., *Phys. Rev. Lett.*, **89** (2002) 137904.
[30] Dong R., Lassen M., Heersink J., Marquardt C., Filip R., Leuchs G. and Andersen U. L., *Nat. Phys.*, **4** (2008) 919.
[31] Aoki T., Takahashi G., Kajiya T., Yoshikawa J., Braunstein S. L., van Loock P. and Furusawa A., *Nat. Phys.*, **5** (2009) 541.
[32] Cerf N. J., Krüger O., Navez P., Werner R. F. and Wolf M. M., *Phys. Rev. Lett.*, **95** (2005) 070501.
[33] Casagrande F., Lulli A. and Paris M. G. A., *Phys. Rev. A*, **75** (2007) 032336.
[34] Sasaki M. and Suzuki S., *Phys. Rev. A*, **73** (2006) 043807.
[35] Ourjoumtsev A., Dantan A., Tualle-Brouri R. and Grangier P., *Phys. Rev. Lett.*, **98** (2007) 030502.
[36] O'Sullivan M. N., Clifford Chan K. W., Lakshminarayanan V. and Boyd R. W., *Phys. Rev. A*, **77** (2008) 023804.
[37] Takahashi H., Neergaard-Nielsen J. S., Takeuchi M., Takeoka M., Hayasaka K., Furusawa A. and Sasaki M., *Nat. Photonics*, **4** (2010) 178.
[38] Braczyk A. M., Ralph T. C., Helwig W. and Silberhorn C., *New J. Phys.*, **12** (2010) 063001.
[39] Gerrits T., Glancy S., Clement T. S., Calkins B., Lita A. E., Miller A. J., Migdall A. L., Nam S. W., Mirin R. P. and Knill E., arXiv:1004.2727v1.
[40] Genoni M. G., Beduini F. A., Allevi A., Bondani M., Olivares S. and Paris M. G. A., *Phys. Scr.*, **T140** (2010) 014007.
[41] Agliati A., Bondani M., Andreoni A., De Cillis G. and Paris M. G. A., *J. Opt. B*, **7** (2005) 652.
[42] Wasilewski W., Lvovsky A. I., Banaszek K. and Radzewicz C., *Phys. Rev. A*, **73** (2006) 063819.
[43] Bondani M., Allevi A., Zambra G., Paris M. G. A. and Andreoni A., *Phys. Rev. A*, **76** (2007) 013833.
[44] Lvovsky A. I., Wasilewski W. and Banaszek K., *J. Mod. Opt.*, **54** (2007) 721.
[45] Wasilewski W., Radzewicz C., Frankowski R. and Banaszek K., *Phys. Rev. A*, **78** (2008) 033831.
[46] Mauerer W., Avenhaus M., Helwig W. and Silberhorn C., *Phys. Rev. A*, **80** (2009) 053815.
[47] Helwig W., Mauerer W. and Silberhorn C., *Phys. Rev. A*, **80** (2009) 052326.
[48] Söller C., Brecht B., Mosley P. J., Zang L. Y., Podlipensky A., Joly N. Y., Russell P. St. J. and Silberhorn C., *Phys. Rev. A*, **81** (2010) 031801.
[49] Bondani M., Allevi A., Agliati A. and Andreoni A., *J. Mod. Opt.*, **56** (2009) 226.
[50] Paleari F., Andreoni A., Zambra G. and Bondani M., *Opt. Express*, **12** (2004) 2816.
[51] Bondani M., Allevi A. and Andreoni A., *Adv. Sci. Lett.*, **2** (2009) 463; *Opt. Lett.*, **34** (2009) 1444.
[52] Allevi A., Bondani M. and Andreoni A., *Opt. Lett.*, **35** (2010) 1707.
[53] Andreoni A. and Bondani M., *Phys. Rev. A*, **80** (2009) 013819.
[54] Genoni M. G., Paris M. G. A. and Banaszek K., *Phys. Rev. A*, **76** (2007) 042327; **78** (2008) 060303(R).
[55] Genoni M. G., Invernizzi C. and Paris M. G. A., *Phys. Rev. A*, **80** (2009) 033842.
[56] Mosley P. J., Christ A., Eckstein A. and Silberhorn C., *Phys. Rev. Lett.*, **103** (2009) 233901.